

Evolution of the $7/2$ fractional quantum Hall state in two-subband systems

Yang Liu, J. Shabani, D. Kamburov, M. Shayegan, L.N. Pfeiffer, K.W. West, and K.W. Baldwin
Department of Electrical Engineering, Princeton University, Princeton, New Jersey 08544

(Dated: September 8, 2011)

We report the evolution of the fractional quantum Hall state (FQHS) at even-denominator filling factor $\nu = 7/2$ in wide GaAs quantum wells in which electrons occupy two electric subbands. The data reveal subtle and distinct evolutions as a function of density, magnetic field tilt-angle, or symmetry of the charge distribution. When the charge distribution is strongly asymmetric, there is a remarkable persistence of a resistance minimum near $\nu = 7/2$ when two Landau levels belonging to the two subbands cross at the Fermi energy. The field position of this minimum tracks the $5/2$ filling of the symmetric subband, suggesting a pinning of the crossing levels and a developing $5/2$ FQHS in the symmetric subband even when the antisymmetric level is partially filled.

The fractional quantum Hall states (FQHSs) at the even-denominator Landau level (LL) filling factors [1] have recently come into the limelight thanks to the theoretical prediction that these states might be non-Abelian [2] and be useful for topological quantum computing [3]. This expectation has spawned a flurry of investigations, both experimental [4–10] and theoretical [11–13], into the origin and stability of the even-denominator states. Much of the attention has been focused on the $\nu = 5/2$ FQHS which is observed in very low disorder two-dimensional electron systems (2DESs) when the Fermi energy (E_F) lies in the spin-up, excited-state ($N = 1$), LL of the ground-state (symmetric, S) electric subband of the 2DES, namely in the $S1\uparrow$ level. Here we examine the stability of the FQHS at $\nu = 7/2$, another even-denominator FQHS, typically observed when E_F is in the $S1\downarrow$ level (Fig. 1(a)) [4, 7]. The $\nu = 7/2$ FQHS, being related to the $5/2$ state through particle-hole symmetry, is also theoretically expected to be non-Abelian. Our study, motivated by theoretical proposals that the even-denominator FQHSs might be favored in 2DESs with "thick" wavefunctions [11–13], is focused on electrons confined to wide GaAs quantum wells (QWs). In a realistic, experimentally achievable wide QW, however, the electrons at $\nu = 7/2$ can occupy the second (antisymmetric, A) electric subband when the subband energy spacing (Δ) is comparable to the cyclotron energy $\hbar\omega_c$ (Figs. 1(b-d)). Here we experimentally probe the stability of the $\nu = 7/2$ FQHS in wide QW samples with tunable density in the vicinity of the crossings (at E_F) between the $S1$ and the $A0$ LLs.

Our samples were grown by molecular beam epitaxy, and each consist of a wide GaAs QW bounded on each side by undoped $\text{Al}_{0.24}\text{Ga}_{0.76}\text{As}$ spacer layers and Si δ -doped layers. We report here data, taken at $T \simeq 30$ mK, for three samples with QW widths of $W = 37, 42$, and 55 nm. The QW width and electron density (n) of each sample were designed so that its Δ is close to $\hbar\omega_c$ at the magnetic field position of $\nu = 7/2$. This enables us to make the $S1$ and the $A0$ LLs cross at E_F by tuning n or the charge distribution asymmetry, which we achieve by applying back- and front-gate biases [7, 14–16]. For each

n , we measure the occupied subband electron densities n_S and n_A from the Fourier transforms of the low-field ($B \leq 0.5$ T) Shubnikov-de Haas oscillations [14, 15], and determine $\Delta = (\pi\hbar^2/m^*)(n_S - n_A)$, where $m^* = 0.067m_e$ is the GaAs electron effective mass. At a fixed total density, Δ is smallest when the charge distribution is "balanced" (symmetric) and it increases as the QW is imbalanced. Our measured Δ agree well with the results of calculations that solve the Poisson and Schroedinger equations to obtain the potential energy and the charge distribution self-consistently (see, e.g., Figs. 1(a,d)).

Figure 1 shows a series of longitudinal (R_{xx}) and Hall (R_{xy}) resistance traces in the range $3 < \nu < 4$ for a 42 nm-wide QW sample, taken at different n from 2.13 to $2.96 \times 10^{11} \text{ cm}^{-2}$ while keeping the total charge distribution balanced. As n is increased in this range, Δ decreases from 64 to 54 K while $\hbar\omega_c$ at $\nu = 7/2$ increases from 50 K to 70 K, so we expect crossings between the $S1$ and $A0$ levels, as illustrated in Figs. 1(a-d). These crossings manifest themselves in a remarkable evolution of the FQHSs as seen in Fig. 1. At the lowest n , which corresponds to the LL diagram shown in Fig. 1(a), R_{xx} shows a reasonably deep minimum at $\nu = 7/2$, accompanied by a clear inflection point in R_{xy} at $7/2(h/e^2)$, and a weak minimum near $\nu = 10/3$. These features are characteristic of the FQHSs observed in high-quality, standard (single-subband) GaAs 2DESs, when E_F lies in the $S1\downarrow$ LL [4, 7]. As n is raised, we observe an R_{xx} spike near $\nu = 7/2$, signaling a crossing of $S1\downarrow$ and $A0\uparrow$. At $n = 2.51 \times 10^{11} \text{ cm}^{-2}$, these levels have crossed, and E_F is now in $A0\uparrow$ (Fig. 1(b)). There is no longer a minimum at $\nu = 7/2$ and instead, there are very strong minima at $\nu = 10/3$ and $11/3$. Further increasing n causes a crossing of $S1\uparrow$ and $A0\uparrow$ and, at $n = 2.63 \times 10^{11} \text{ cm}^{-2}$, E_F at $\nu = 7/2$ lies in $S1\uparrow$ (Fig. 1(c)). Here the R_{xx} minimum and R_{xx} inflection point at $\nu = 7/2$ reappear, signaling the return of a FQHS. As we increase n even further, $S1\uparrow$ and $A0\downarrow$ cross and, at $n = 2.96 \times 10^{11} \text{ cm}^{-2}$, when E_F at $\nu = 7/2$ lies in $A0\downarrow$, there is again no $\nu = 7/2$ minimum but there are strong FQHSs at $\nu = 10/3$ and $11/3$.

The above observations provide clear and direct evidence that the even-denominator $\nu = 7/2$ FQHS is stable

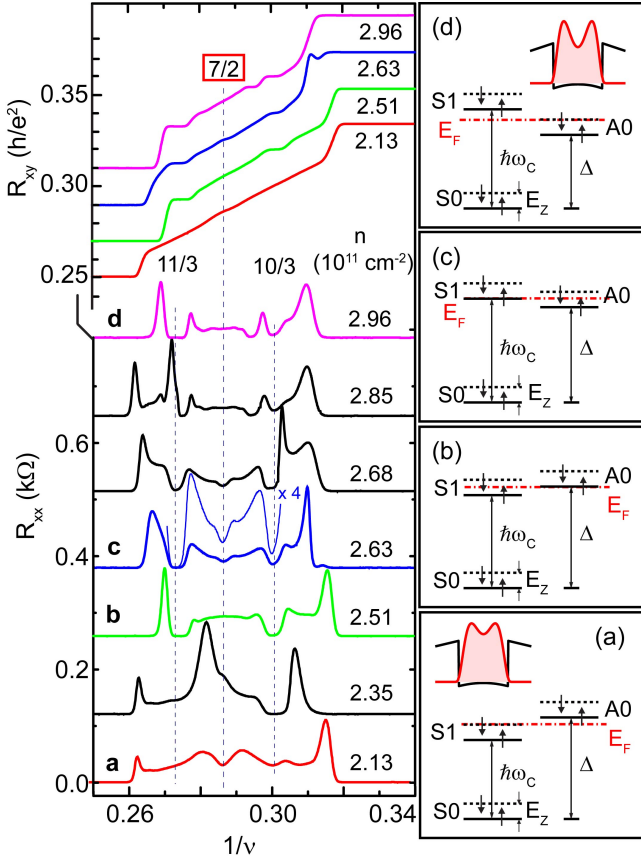


FIG. 1. (color online) Left panel: Waterfall plot of R_{xx} and R_{xy} traces at different densities for a 42-nm-wide GaAs QW. (a-d) LL diagrams at $\nu = 7/2$ for different densities. Self-consistently calculated charge distributions are shown in the insets to (a) and (d) for $n = 2.13$ and $2.96 \times 10^{11} \text{ cm}^{-2}$.

when E_F is in an excited ($N = 1$) LL but not when E_F lies in a ground-state ($N = 0$) LL [7]. Examining traces taken at numerous other n , not shown in Fig. 1 for lack of space, reveal that the appearances and disappearances of the $\nu = 7/2$ FQHS are sharp, similar to the behavior of the $5/2$ FQHS at a LL crossing [17]. It is noteworthy that when the two crossing levels have *antiparallel* spins, a "spike" in R_{xx} at the crossing completely destroys the FQHS at $\nu = 7/2$ and nearby fillings. At the crossing of two levels with *parallel* spins, on the other hand, there is no R_{xx} spike. These behaviors are reminiscent of easy-axis and easy-plane ferromagnetism for the antiparallel- and parallel-spin crossings, respectively [16, 18].

Next, we examine the evolution of the $\nu = 7/2$ FQHS in the presence of a parallel magnetic field component $B_{||}$, introduced by tilting the sample so that its normal makes an angle θ with the total field direction (Fig. 2(b)). Figure 2(a) captures this evolution for electrons confined to a symmetric, 37-nm-wide QW [19]. This QW is narrower so that, at $n = 2.34 \times 10^{11} \text{ cm}^{-2}$, its Δ ($= 82 \text{ K}$) is well above $\hbar\omega_c$ ($= 55 \text{ K}$). The $\theta = 0$ trace then corresponds to E_F lying in $S1\downarrow$, as shown in Fig. 2(d). As θ is increased,

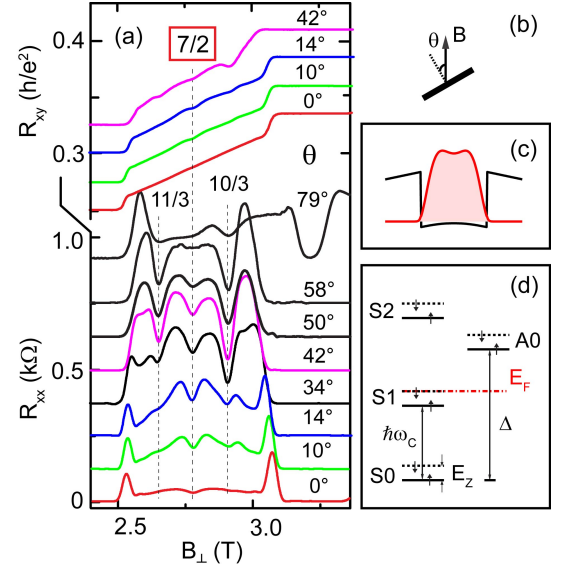


FIG. 2. (color online) (a) R_{xx} and R_{xy} traces for a 37-nm-wide GaAs QW at $n = 2.34 \times 10^{11} \text{ cm}^{-2}$ at different tilt angles θ as depicted in (b). (c) Charge distribution calculated self-consistently at $B = 0$. (d) LL diagram at $\theta = 0$ at $\nu = 7/2$.

we observe only a gradual change in the strength of the $\nu = 7/2$ FQHS, until it disappears at large $\theta \gtrsim 55^\circ$. This is not surprising since, in a two-subband system like ours, we expect a severe mixing of the LLs of the two subbands with increasing θ [20] rather than sharp LL crossings as manifested in Fig. 1 data.

We highlight three noteworthy features of Fig. 2 data. First, the $\nu = 7/2$ R_{xx} minimum persists up to relatively large θ (up to 50°), and it even appears that the R_{xy} plateau is better developed at finite θ (up to $\theta = 42^\circ$) compared to $\theta = 0$, suggesting a strengthening of the $7/2$ FQHS at intermediate angles. Second, deep R_{xx} minima develop with increasing θ at $\nu = 10/3$ and $11/3$, suggesting the development of reasonably strong FQHSs at these fillings. This is consistent with the results of Xia *et al.* who report a similar strengthening of the $7/3$ and $8/3$ states - the equivalent FQHSs flanking the $\nu = 5/2$ state in the $S1\uparrow$ level - when a wide QW sample is tilted in field [9]. Third, the large magnitude of $B_{||}$ at the highest angles appears to greatly suppress Δ [21], rendering the electron system essentially into a bilayer system. This is evidenced by the dramatic decrease in the strength of the $\nu = 3$ QHS and the disappearance of the $\nu = 11/3$ R_{xx} minimum at $\theta = 79^\circ$; note that a FQHS should not exist at $\nu = 11/3$ in a bilayer system with two isolated 2DESS as it would correspond to $11/6$ filling in each layer.

We now focus on data taken on a 55-nm-wide QW where we keep the total n fixed and change the charge distribution symmetry by applying back- and front-gate biases with opposite polarity. In Fig. 3(a) we show a set of R_{xx} traces, each taken at a different amount of asym-

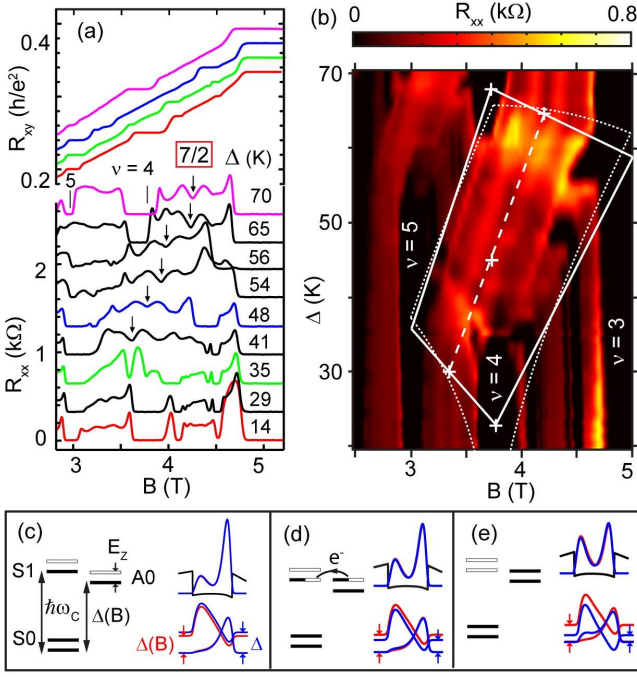


FIG. 3. (color online) (a) R_{xx} and R_{xy} traces for a 55-nm-wide GaAs QW at a fixed $n = 3.62 \times 10^{11} \text{ cm}^{-2}$, as the charge distribution is made increasingly asymmetric. Values of Δ , measured from low- B Shubnikov-de Haas oscillations, are indicated for each trace. Vertical arrows mark the positions of observed anomalous R_{xx} minima. (b) A color-scale plot of data in (a). Solid and dotted lines are the calculated boundary within which the $S1\uparrow$ and $A0\uparrow$ levels are pinned together at E_F . The dashed line represents the values of B at which, according to the calculations, the $S1\uparrow$ level is half-filled; it tracks the positions of the observed R_{xx} minima marked by vertical arrows in (a). (c-e) Schematic LL diagrams (left) and charge distributions and wavefunctions (right), self-consistently calculated at $B = 0$ (blue) and at $\nu = 4$ (red). In (c-e), the filling factor of the $S1\uparrow$ level equals 1, 0.5, and 0, respectively. In each panel, the calculated wavefunctions are shifted vertically according to the calculated values of Δ and $\Delta(B)$.

metry. The measured Δ is indicated for each trace and ranges from 14 K for the symmetric charge distribution to 70 K for a highly asymmetric distribution. In Fig. 3(b) we present a color-scale plot of R_{xx} with B and Δ as x and y axes, based on an interpolation of Fig. 3(a) data and many other traces taken at different values of Δ . When the charge distribution is symmetric or nearly symmetric in this QW, Δ is much smaller than $\hbar\omega_c$ ($= 85 \text{ K}$ at $\nu = 7/2$) so that the LL diagram is qualitatively the one shown in Fig. 1(d). Consistent with this LL diagram, we observe a very strong $\nu = 4$ QHS. Also, since E_F lies in the $A0\downarrow$ level at $\nu = 7/2$, there is no $\nu = 7/2$ FQHS and instead we observe strong FQHSs at $\nu = 10/3$ and $11/3$. As Δ is increased, we expect a crossing of $S1\uparrow$ and $A0\downarrow$, leading to a destruction of the $\nu = 4$ QHS at the crossing. This is indeed seen in Figs. 3(a) and (b). What is striking, however, is that the $\nu = 4$ R_{xx} mini-

mum disappears over a very large range of Δ , between 35 and 62 K. Even more remarkable are several anomalous R_{xx} minima in this range of Δ in the filling range $3 < \nu < 5$, particularly those marked by arrows in Fig. 3(a). These minima resemble what is observed in the top trace but are seen at lower fields.

These features betray a pinning together, at E_F , of the partially occupied $S1\uparrow$ and $A0\downarrow$ levels, and a charge transfer between them, in a finite range of B and gate bias. As pointed out in Ref. [22], when only a small number of quantized LLs belonging to two different subbands are occupied, the distribution of electrons between these levels does not necessarily match the $B = 0$ subband densities. This leads to a mismatch between the total electron charge density distributions at $B = 0$ and high B . The pinning and the inter-LL charge transfer help bring these distributions closer to each other [22, 23]. To demonstrate such a pinning quantitatively and determine the boundary inside which the $S1\uparrow$ and $A0\downarrow$ levels are pinned together, we performed self-consistent calculations of the potential energy and charge distribution at high B , similar to those described in Ref. [22]. This boundary is marked by solid lines in Fig. 3(b).

First, we assume that one point at this boundary, corresponding to $A0\downarrow$ having just moved above $S1\uparrow$ at $\nu = 7/2$ so that $S1\uparrow$ is half-filled and $A0\downarrow$ is empty, occurs at $\Delta = 65 \text{ K}$. The rationale is that, for $\Delta = 65 \text{ K}$, the $B = 0$ subband density ratio $n_S/n_A = 2.5$ is equal to the ratio of fillings $\nu_S/\nu_A (= 2.5/1.0)$ for the S and A subbands at $\nu = 7/2$. Note in Fig. 3 that the trace taken at $\Delta = 65 \text{ K}$ indeed shows a strong minimum at total $\nu = 7/2$ but traces taken at lower Δ do not. This is consistent with our assumption that $\Delta \simeq 65 \text{ K}$ marks the onset of full depopulation of $A0\uparrow$. Now, since the onset occurs when $\Delta = \hbar\omega_c - E_Z$, we conclude that $E_Z \simeq 21 \text{ K}$, implying an effective g -factor $\simeq 7.3$, which is 17-fold enhanced over the GaAs band value (0.44); this is similar to the enhancements observed for electrons confined to similar wide QWs [16].

Next, we assume that in the region where the pinning occurs, g has a fixed value of 7.3 [24], and that the *in-field* subband separation is given by $\Delta(B) = \hbar\omega_c - E_Z$. This expression ensures that $\Delta(B)$ is fixed at a given B , consistent with the pinning of the $S1\uparrow$ and $A0\downarrow$ levels. We then perform *in-field* self-consistent calculations for a series different QW asymmetries. For each QW asymmetry, the *in-field* charge distribution is given by:

$$\rho(B) = e(eB/h)[\nu_S \cdot |\psi_S(B)|^2 + \nu_A \cdot |\psi_A(B)|^2]. \quad (1)$$

Now, for the different points on the boundary, ν_S and ν_A have specific and well-defined values. For example, at $\nu = 4$ ($B = 3.75 \text{ T}$), for which we show the results of our self-consistent calculations in Figs. 3(c) and (e), we have $\nu_S = 3$ and $\nu_A = 1$ for the upper boundary and $\nu_S = \nu_A = 2$ for the lower one. Focusing on the upper boundary, i.e., using $\nu_S = 3$ and $\nu_A = 1$ in Eq. (1),

among all the QW asymmetries for which we perform the self-consistent calculations, one in particular has a subband separation which is equal to $\Delta(B)$ ($= 56$ K for $B = 3.75$ T). This particular QW asymmetry gives the upper boundary at $B = 3.75$ T. We then calculate the zero-field subband separation for this asymmetry, which turns out to be $\Delta = 68$ K, and mark it in Fig. 3(b) as the upper boundary for the pinning at $B = 3.75$ T. For the lower boundary at $B = 3.75$ T, we repeat the above calculations using $\nu_S = \nu_A = 2$. The QW asymmetry that gives $\Delta(B) = 56$ K yields a zero-field Δ of 23 K which we mark in Fig. 3(b) as the lower boundary at 3.75 T. The rest of the boundary in Fig. 3(b) is determined in a similar fashion. For example, the upper boundary at $\nu = 7/2$ corresponds to ($\nu_S = 2.5$, $\nu_A = 1$) and the lower boundary to ($\nu_S = 2$, $\nu_A = 1.5$).

It is clear that the calculated boundary marked by the solid lines in Fig. 3(b) matches well the region (in Δ vs. B plane) in which we experimentally observe a disappearance of the $\nu = 4$ R_{xx} minimum and the appearance of R_{xx} minima at anomalous fillings. This matching is particularly remarkable, considering that there are no adjustable parameters in our simulations, except for using a single value (7.3) for the enhanced g -factor [24]. In Fig. 3(b) we also include a dashed line representing the values of B at which, according to our calculations, the $S1\uparrow$ level is exactly half-filled, i.e., $\nu_S = 5/2$ and $\nu_A = (\nu - 5/2)$. This dashed line tracks the positions of the observed R_{xx} minima marked by vertical arrows in (a) very well, suggesting that these minima indeed correspond to $\nu_S = 5/2$. This is an astonishing observation, as it implies that there is a developing FQHS at $5/2$ filling of the symmetric subband even when a partially filled $A0\downarrow$ level is pinned to the half-filled $S1\uparrow$ level at E_F !

In Fig. 3(b) we also show a boundary, marked by dotted lines, which is based on a simple, *analytic* model. Note that the simulations shown in Figs. 3(c-e) indicate that the in-field charge distributions, calculated self-consistently at $\nu = 4$, are nearly the same as the $B = 0$ distributions. In our simple model, we assume that the in-field wavefunctions $\psi_S(B)$ and $\psi_A(B)$ are just linear combinations of the $B = 0$ wavefunctions $\psi_S(0)$ and $\psi_A(0)$. We then set the total in-field charge distribution, given by Eq. (1), equal to its $B = 0$ value, $\rho(0) = en_S|\psi_S(0)|^2 + en_A|\psi_A(0)|^2$, and find:

$$\Delta_0^2 = (\nu_S - \nu_A)(eB/h)(\pi\hbar^2/m^*)\Delta(B). \quad (2)$$

For a given value of B and therefore $\Delta(B) = \hbar\omega_c - E_Z$, Eq. (2) gives the $B = 0$ subband separation Δ_0 which corresponds to the onset of pinning/depinning of the relevant LLs. For example, to find the upper boundary at $B = 4$ T ($\nu = 3.75$), we use $\Delta(B) = 60$ K, $\nu_A = 1$ and $\nu_S = 2.75$, and solve Eq. (2) to find $\Delta_0 = 65$ K. To find the lower boundary at $B = 4$ T, we use $\nu_S = 2$ and $\nu_A = 1.75$ and find $\Delta_0 = 25$ K. As seen in Fig. 3(b), the dotted line given by the simple, analytic expres-

sion (2) matches the boundary determined from in-field self-consistent calculations reasonably well except for the lower points where $\nu_S = \nu_A \simeq 2$ leads to $\Delta_0 \simeq 0$.

In summary our results reveal distinct metamorphoses of the ground-state of two-subband 2DEs at and near $\nu = 7/2$ as either the field is tilted, or the density or the charge distribution symmetry are varied. Most remarkably, we observe a developing FQHS when a half-filled $S1\uparrow$ level is pinned to a partially-filled $A0\downarrow$ level [25].

We acknowledge support through the DOE BES (DE-FG0200-ER45841) for measurements, and the Moore Foundation and the NSF (DMR-0904117 and MRSEC DMR-0819860) for sample fabrication and characterization. A portion of this work was performed at the National High Magnetic Field Laboratory, which is supported by the NSF, DOE, and the State of Florida.

-
- [1] R. L. Willett *et al.*, Phys. Rev. Lett. **59**, 1776 (1987).
 - [2] G. Moore and N. Read, Nuclear Physics B **360**, 362 (1991).
 - [3] C. Nayak *et al.*, Rev. Mod. Phys. **80**, 1083 (2008).
 - [4] C. R. Dean *et al.*, Phys. Rev. Lett. **100**, 146803 (2008).
 - [5] H. C. Choi *et al.*, Phys. Rev. B **77**, 081301 (2008).
 - [6] J. Nuebler *et al.*, Phys. Rev. B **81**, 035316 (2010).
 - [7] J. Shabani *et al.*, Phys. Rev. Lett. **105**, 246805 (2010).
 - [8] A. Kumar *et al.*, Phys. Rev. Lett. **105**, 246808 (2010).
 - [9] J. Xia *et al.*, Phys. Rev. Lett. **105**, 176807 (2010).
 - [10] W. Pan *et al.*, Phys. Rev. Lett. **106**, 206806 (2011).
 - [11] E. H. Rezayi and F. D. M. Haldane, Phys. Rev. Lett. **84**, 4685 (2000).
 - [12] M. R. Peterson *et al.*, Phys. Rev. Lett. **101**, 016807 (2008); Phys. Rev. B **78**, 155308 (2008).
 - [13] A. Wójs *et al.*, Phys. Rev. Lett. **105**, 096802 (2010).
 - [14] Y. W. Suen *et al.*, Phys. Rev. Lett. **72**, 3405 (1994).
 - [15] J. Shabani *et al.*, Phys. Rev. Lett. **103**, 256802 (2009).
 - [16] Y. Liu *et al.*, arXiv:1102.0070 (2011).
 - [17] Y. Liu *et al.*, arXiv:1106.0089 (2011).
 - [18] K. Muraki *et al.*, Phys. Rev. Lett. **87**, 196801 (2001).
 - [19] Application of a $B_{||}$ component leads to an anisotropic state at intermediate tilt angles. Traces shown in Fig. 2 were taken along the hard-axis; data along the easy-axis show a qualitatively similar behavior.
 - [20] N. Kumada *et al.*, Phys. Rev. B **77**, 155324 (2008).
 - [21] J. Hu and A. H. MacDonald, Phys. Rev. B **46**, 12554 (1992).
 - [22] S. Trott *et al.*, Phys. Rev. B **39**, 10232 (1989).
 - [23] A. G. Davies *et al.*, Phys. Rev. B **54**, R17331 (1996); V. V. Solov'yev *et al.*, **80**, 241310 (2009).
 - [24] The fact that the boundary we calculate based on $g = 7.3$ matches the region where the pinning is observed validates our choice of this value. A full many-body calculation that takes exchange interaction and variations of g with B and wavefunction asymmetry into account might explain the experimental observations more accurately.
 - [25] J. Nuebler *et al.* independently made a similar observation, that a FQHS exists when the $S1\uparrow$ level is half filled while the $A0\uparrow$ level is partially occupied (unpublished).